Research on MPPT and Single-Stage Grid-Connected for Photovoltaic System

JUI-LIANG YANG, DING-TSAIR SU, YING-SHING SHIAO
Department of Electrical Engineering
National Chang-hua University of Education
Bao-Shan Campus, Address: No.2, Shi-Da Road, Changhua City 520
REPUBLIC OF CHINA.(TAIWAN)
y5111@mail.elvs.chc.edu.tw, sdt@cc.ctu.edu.tw, shiaoing@cc.ncue.edu.tw
http://www.ncue.edu.tw

Abstract: - This paper proposes a grid-connected photovoltaic (PV) system that is consisted of a boost converter with maximum power tracking, battery charge controller, inverter, and the related control circuits. A sliding mode controller is designed for controlling the boost converter to output the maximum power of the solar cells. A control strategy is proposed of a Maximum Power Point Tracking (MPPT) impendence adapter coupling a photovoltaic generator to a battery. The proposed strategy is based on the sliding mode control theory of continuing systems to permit a direct control of power converter. The PV generator price is even relatively high, so the user is interested of the optimal coupling of PV generator to electromechanical loads. In fact, this system uses the optimal coupling in order to have maximum power during the whole operating period.

A grid-connected inverter is designed to transform the maximum output power into the load and utility. The real power control is using zero-cross and phase-lock circuits that control the inverter output voltage which is phase lead and synchronized with the utility. A digital circuit is used to detect the phase angles of the load voltage and current to control the inverter output amplitude to achieve the reactive power load compensation. A monitor circuit is designed to detect the voltage and frequency variation in the utility. When the photovoltaic system encounters a voltage and frequency deviation, the monitor circuit immediately disconnects the photovoltaic system from the utility to prevent the island effect. The proposed system is implemented by using OP amplifiers and micro controller (PIC16F877A). Both the simulation and experimental results using MATLAB show the sliding mode controller for maximum power tracking has good performance. The phase and amplitude control experiments achieve the real and reactive power control. The island effect experiments demonstrate evidence of the solar cell system protection ability illustrating the proposed grid-connected photovoltaic system has good operating performance.

Key-Words: - MPPT, Sliding mode control, Battery charger, Lyapunov function, Boost converter

1 Introduction

Due to depletion of fossil energy and environmental contamination, a renewable energy application such as photovoltaic (PV) system has been widely used for a few decades. The PV energy is free, abundant and distributed through the earth. Photovoltaic (PV) systems are solar energy supply systems, which either supply power directly to electrical equipment or feed energy into the public electricity grid. Generally, photovoltaics are considered as an expensive method of producing electricity. Moreover, with the developing of PV technologies, application of photovoltaic in grid-connected situations has grown rapidly, which shows that photovoltaic are very attractive to pro- duce environmentally benign electricity for diversified purpose [1-3]. Among the PV energy applications, they can be divided into two categories: one is stand-alone system and the other is grid-connected system. Stand-alone system requires the battery bank to store the PV energy which is suitable for low-power system. On the other hands, grid-connected system does not require the battery bank and has become the primary PV application for high power applications. The main purpose of the grid-connected system is to transfer maximum solar array energy into grid with a unity power factor.

The output power of PV cell is changed by environmental factors, such as illumination and temperature. Since the characteristic curve of a solar cell exhibits a nonlinear voltage-current characteristic, a controller named maximum power point tracker (MPPT) is required to match the solar cell power to the environmental changes. Many algorithms have been developed for tracking maximum power point of a solar cell. In recent years, the research of the PV MPPT control methods has been paid extensive attention by many specialist and obtained some fruits such as: P&O and fuzzy control etc. Because the output energy of the PV arrays

changes frequently by the surroundings, improving the speed of tracking the PV power system could obviously improve the system performance.

The existing tracking control methods for the MPPT can be classified into five categories: (i.) hill-climbing [1] / perturb and observe (P&O) [2]-[4]. The system then oscillates about the MPP. The oscillation can be minimized by reducing the perturbation step size. However, a smaller perturbation size slows down the MPPT. Hill-climbing can fail under rapidly changing atmospheric conditions. (ii.) incremental conductance [5-6]; (iii.) open-circuit voltage and short-circuit current [7-9]; (iv.) fuzzy logic control [10]; and (v) neural network control [11]. X. Li et al. introduced the fuzzy tracking control approaches [10] in 2002. But it is very difficult to formulate the fuzzy rules, which are usually obtained from the trial-and-error procedure. In 2006, the computational expensive neural network was adopted by Tariq et al. [11]. The algorithm requires on-line learning in order to make the robot perform properly.

In this paper, we propose a grid-connected photovoltaic system that is consisted of a boost converter with maximum power tracking, battery charge controller, inverter, and the required control circuits. we come up with sliding mode control strategy [12-16] to solve the problem of MPPT under the condition of all kinds of radiation levels. A grid-connected inverter [4] is designed to transform the maximum output power into the load and utility. The real power control is realized using zero-cross and phase-lock circuits that control the inverter output voltage which is phase lead and synchronized with the utility. A digital circuit is used to detect the phase angles of the load voltage and current to control the inverter output amplitude to achieve the reactive power load compensation. A monitor circuit is designed to detect the voltage and frequency variation in the utility. When the photovoltaic system encounters a voltage and frequency deviation, the monitor circuit immediately disconnects the photovoltaic system from the utility to prevent the island effect. This paper is organized as follows. The DC-DC analysis and mathematical modeling are presented in Section 2, and Section 3 aims at the MPPT controller design. Section 4 is focused on the charge controller design. Section 5 is devoted to the grid connected Photovoltaic system. simulation and experimental results are presented in section 6. In Section 7 concludes this paper.

2 The Boost Converter of Analysis and Mathematical Modeling

The output energy of the PV arrays is influenced by the surrounding, such as the surrounding temperature, the solar radiation and the terminal voltage of PV arrays etc, the PV arrays characteristic curve is shown as Fig.1. Mathematical model of the solar array can be expresses as Equ. (1) [17][18].

$$I = I_g - I_{sat}\left[\exp(\frac{q}{AKT}V) - 1\right] \quad (1)$$

where I_g denotes a current of a solar array, V denotes an output voltage of a solar array, q denotes an electron charge (C) , I_{sat} denotes a cell reverse saturation current (A), K is the Boltzman's constant (J/K), T is a cell temperature (K), A denotes the ideality factor ◦

In order to charger the battery, the PV MPPT system adopt step up type DC-DC converter topology system. Fig. 2 presents its system structure. Fig. 2 shows the Boost Converter to transfer power to load from solar array. In the Fig.2, D represents the switch function of the power switch device to control the output energy of the solar array. When $D=0$, power will be switched to open. When $D=1$, power will be switched to close. From Fig.2, we can draw the system dynamic model as follows.

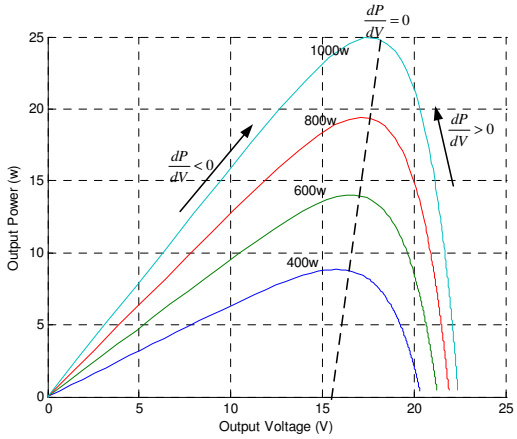

Fig.1 The PV arrays characteristic

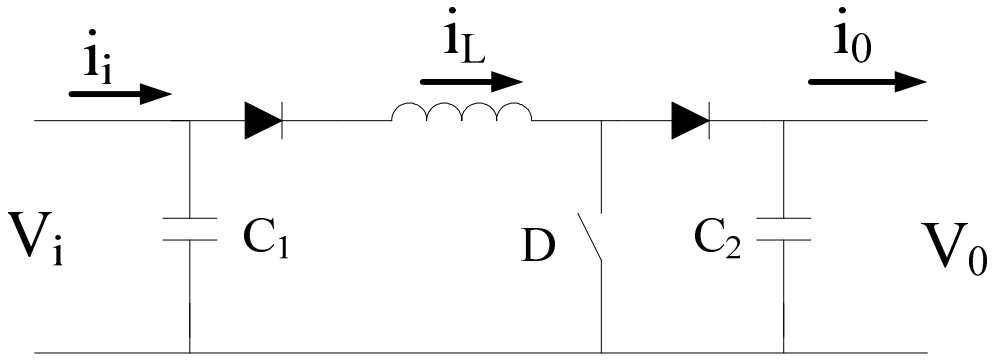

Fig. 2 The circuit diagram of PV DC-DC converter system

$$\begin{cases} V_i = L\dfrac{di_L}{dt} + (1-D)V_0 \\ i_L = i_i - C_1\dfrac{dV_i}{dt} \\ i_0 = (1-D)i_L - C_2\dfrac{dV_0}{dt} \end{cases} \tag{2}$$

$$\begin{cases} \dot{V}_i = (i_i - i_L)/C_1 \\ \dot{i}_L = -\dfrac{1}{L}(1-D)V_0 + \dfrac{1}{L}V_i \\ \dot{V}_0 = \dfrac{1}{C_2}(1-D)i_L - \dfrac{1}{C_2}i_0 \end{cases} \tag{3}$$

$$\dot{x} = \begin{bmatrix} \dot{V}_i \\ \dot{i}_L \\ \dot{V}_0 \end{bmatrix}$$

$$f(x) = \begin{bmatrix} (i_i - i_L)/C_1 \\ \dfrac{1}{L}(V_1 - V_0) \\ \dfrac{1}{C_2}(i_L - i_0) \end{bmatrix} \tag{4}$$

$$g(x) = \begin{bmatrix} 0 \\ V_0/L \\ -i_L/C_2 \end{bmatrix}$$

$$\dot{x} = f(x) + g(x)D \tag{5}$$

3 The DC-DC Controller Design

Based on the solar array characteristic curve shown in Fig.1, when the solar array is operating in its maximum output power state, we can get

$$\partial P / \partial V_i = 0 \tag{6}$$

Where (6) represents maximum power achieved.

$$\frac{\partial P}{\partial V_i} = \frac{\partial (V_i i_i)}{\partial V_i} = \frac{\partial i_i}{\partial V_i}V_i + i_i = 0 \tag{7}$$

From (7), the switch function can be selected,

$$S(x) = \frac{\partial P}{\partial V_i} = (\frac{\partial i_i}{\partial V_i}V_i + i_i) \tag{8}$$

Based on the two states of PV arrays in Fig.1 and the system circuit diagram shown as Fig.2, the switch control signal can be selected as

$$D = \begin{cases} 0 & S \geq 0 \\ 1 & S < 0 \end{cases} \tag{9}$$

Let

$$\dot{S} = \frac{\partial S}{\partial x^T}\dot{x} = \frac{\partial S}{\partial x^T}f(x) + \frac{\partial S}{\partial x^T}g(x)D_{eq} = 0 \tag{10}$$

Therefore, the equivalent control variable is shown below.

$$D_{eq} = \frac{i_0}{i_L} \tag{11}$$

Theorem: For the system shown in (5) and the switch function (8), if the expression (9) is adopted, they could make the system eventually stabilize at the status that switch function is equal to zero from any initial state.

Proof:

Let Lyapunov function as

$$V = \frac{1}{2}S^2 > 0 \tag{12}$$

$$\dot{V} = S\frac{dS}{dt} = \frac{dP}{dD_{eq}} \cdot \frac{d}{dt}(\frac{dP}{dD_{eq}})$$

Substituting equation (1) into (8), then

$$S = \frac{\partial P}{\partial V_i} = (\frac{\partial i_i}{V_i}V_i + i_i)$$

$$= I_g - I_{sat}\left[\exp(\frac{qV_i}{AKT}) - 1\right] - \frac{qI_{sat}V_i}{AKT}\exp(\frac{qV_i}{AKT})$$

$$= I_g + I_{sat} - I_{sat}\left[\exp(\frac{qV_i}{AKT})\right] - \frac{qI_{sat}V_i}{AKT}\left[\exp(\frac{qV_i}{AKT})\right]$$

$$= (I_g + I_{sat}) - I_{sat}(1 + \frac{qV_i}{AKT})\left[\exp(\frac{qV_i}{AKT}\right] \tag{13}$$

3.1 When $S > 0$

Base on (8) (9) and Fig. 1, the system is operating in left, the switch function $D = 0$, and V_i is increase.

$$\frac{dVi}{dt} > 0 \tag{14}$$

$$\frac{dS}{dt} = -\frac{qI_{sat}}{AKT}\left[\exp(\frac{qV_i}{AKT})\right]\frac{dV_i}{dt}$$

$$-I_{sat}(1 + \frac{qV_i}{AKT})\left[\exp(\frac{qV_i}{AKT})\right]\frac{q}{AKT}\frac{dV_i}{dt} \tag{15}$$

Bring (14) into (15), then $\frac{dS}{dt} < 0$, so

$$S\frac{dS}{dt} < 0 \tag{16}$$

3.2 When $S < 0$

The system is operating in right, the switch function $D = 1, V_i$ is decreasing, so

$$\frac{dV_i}{dt} < 0 \tag{17}$$

Finally, substituting equation (17) into (15), then $\frac{dS}{dt} > 0$ and $S\frac{dS}{dt} > 0$.

Obviously, the system could reach global stability and the switch function is tending to zero whether the system is operating in left or in right.

3.3 Control Algorithm

The system control rules can be present as follows.

$$D = \begin{cases} 0 & S \geq 0 \\ 1 & S < 0 \end{cases} \tag{18}$$

And the switch functions as:

$$S(x) = \frac{\partial P}{\partial V_i} = (\frac{\partial i_i}{\partial V_i}V_i + i_i) \tag{19}$$

4 The Charge Controller Design

This paper uses pulse charge model to save the power on the lead-acid battery. The pulse width of power transition switch is by the voltage of lead-acid battery to control the charge current. The voltage of battery full-charged for every cell is about 2.43V so that total full-charged battery is about 29.16V.Fig. 3 shows the measurement circuit of lead-acid voltage is measured by current sensor.

The measurement of Battery voltage is put into microchip, PIC16F877A, to control the pulse width of power transition switch and also to control the charge current. As Fig.4 shows, during the current charged, the current generated by booster converter is provided to battery via pulse charge mode. According to the voltage of lead-acid battery and maximum power of solar cell, the battery charged will be the best adjusted.

5 The Grid-Connected Photovoltaic System

This paper proposes the grid-connected photovoltaic system as shown in the Fig.5 which includes solar cell, boost converter and grid-connected inverter. In the grid-connected city power mode, city power is a constant AC and inverter is a voltage source. Therefore, by the technology of Phase-Locked Loop, it will lock the frequency and phase of city power to achieve the synchronization with the city power. The phase and amplitude of output voltage is controlled by inverter to achieve the real power and the reactive power. Besides, in normal condition, SW2 and SW3 are shorted. As the city power is out of order, SW2 and SW3 are off to prevent island effect.

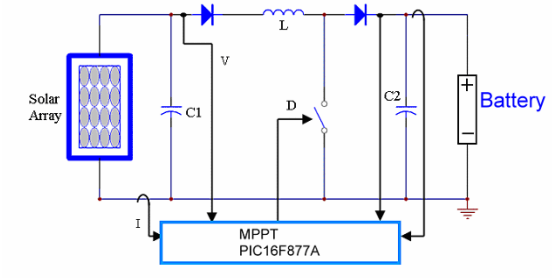

Fig.3 Circuit of Charger Control

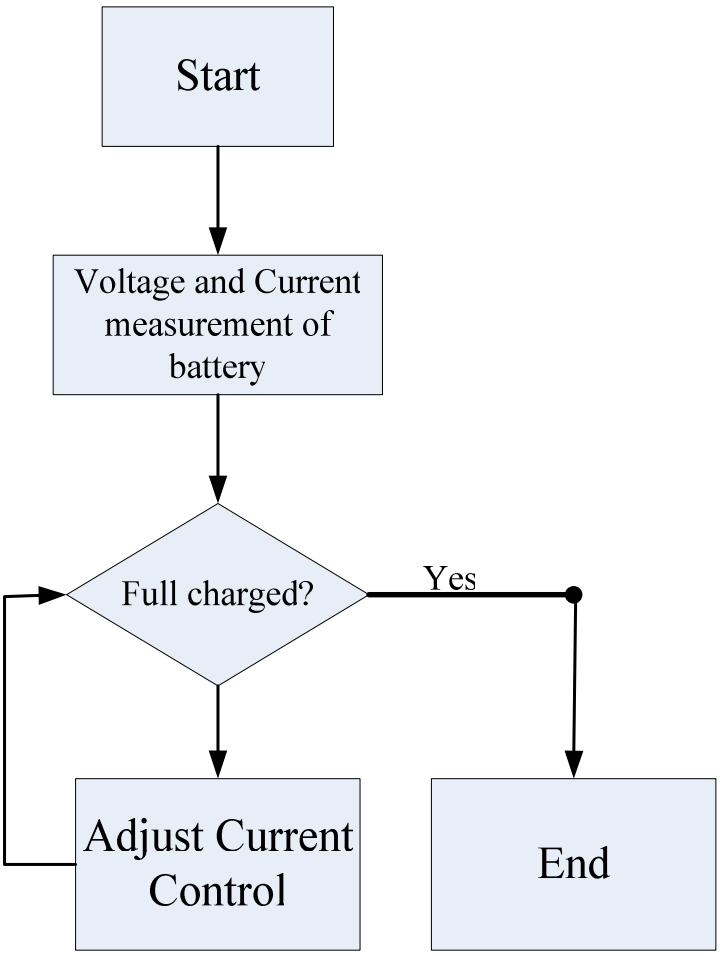

Fig. 4 Flow Chart of Charger Control

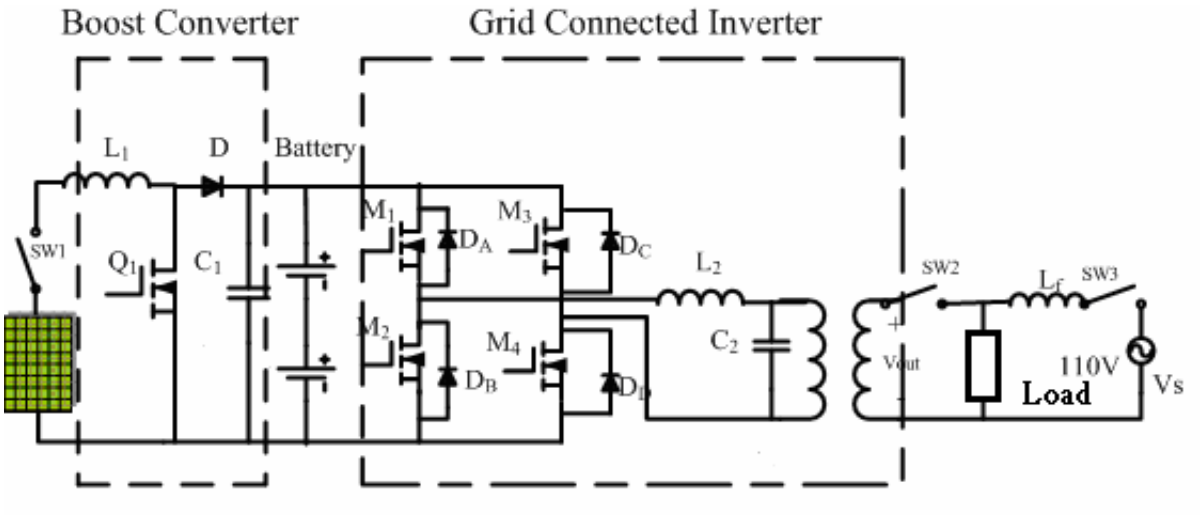

Fig.5 Architecture of Grid Connected Photovoltaic System

5.1 Grid Connection Inverter on Real Power Reactive Power Controller Design

In the Fig.5 grid connection inverter is a single phase full-bridge inverter. When M1 and M4 is shorted, the load of the current is passed from M1 to M4. Similarly, as M2 and M3 are shorted, the load of the current is passed from M2 to M3. By the power switch, M1 ~ M4, the output DC voltage of boost converter is transformed to AC output. The selection on PWM switches frequency of M1~M4 is by the phase-lock circuit and frequency doubler. It uses the frequency, 60Hz, of the city power to raise the frequency to 24kHz and makes the output AC of inverter synchronize with the city power. However, the PWM modulation signal of 24kHz can reduce the value of inductor, L2, and capacitor, C2, of filter. In order to filter the high frequency of PWM to achieve 60Hz, the L2 and Io need to be adjusted.

If the value of the inductor is too small, the value of ripple current gets larger. These will influent both increasing switch and inductor power lost. Also, if the value of the inductor is too large, the dynamic response of inverter will be reduced especially for the non-linear load. Therefore, the selection of capacitor depends on the operation current and switching frequency.

Moreover, the equivalent Series Resistor, ESR, will directly influent the value of output voltage ripples. That is because ESR is one of consumption factor of capacitor. The inner power consumption generates heat and the lifetime of the capacitor is reduced. Therefore, the selection of the capacitor depends on the value of the serial resistor.

So, the frequency selection of inductor and capacitor is less than $\frac{1}{10}$ of f_{pwm} and is greater than 10 times of as shown in Equ. (20).

$$10 * f_{output} \le \frac{1}{2\pi\sqrt{L_f C_f}} \le \frac{f_{PWM}}{10} \tag{20}$$

Parameters for this paper is f_{output} =60Hz, f_{pwm} =24kHz, L2=2mH and C2=5μF.

After the solar cells are traced by boost converter with MPPT, the inverter and the city power will be paralleled. Therefore, output amplitude and phase of inverter will directly influent the real power and reactive power of the city power.

Fig. 5 shows the system circuit for the output voltage control mode of inverter is paralleled with city power.

The city voltage $V_s(t)$ is shown below.

$$V_s(t) = V_m \sin \omega t \tag{21}$$

where V_m is the peak of the city power voltage, ω is the angle frequency of the city power voltage.

The output voltage of grid connection inverter $V_{out}(t)$ is shown below.

$$V_{out}(t) = V_c \sin(\omega t + \delta) \tag{22}$$

Where V_c is the peak of the grid connection inverter. The ω is the angle frequency of grid power. The δ is the phase difference of the grid connection inverter output voltage and city voltage.

The real power of inverter P_S is shown below.

$$P_S = \frac{V_m V_c / \sqrt{2}}{X_f} \sin \sigma \tag{23}$$

The reactive power of inverter Q_S is shown below.

$$Q_S = \frac{V_C / \sqrt{2}}{X_f} \left[V_C / \sqrt{2} - (V_m / \sqrt{2}) \cos \sigma \right] \tag{24}$$

where X_f is inductive reactance of L_f.

By Equ. (23), to control the angle, δ, of $V_S(t)$ can control the P_S, the real power.

By Equ. (24), to control the amplitude, V_C, can control the reactive power, Q_S

.6 Simulation and Experiment Results

6.1 Simulation

This paper used Matlab/Simulink to simulate P&O, fuzzy and sliding mode control. Fig. 7 shows comparison of the tracking maximum power which reveals the sliding mode controller only needs 0.06s, fuzzy controller needs 0.24s and P&O controller needs 1.74s. Therefore, the proposed sliding mode controller is improved its performance of MPPT. Fig. 8 shows the tracking condition of the sliding mode controller as the illumination changes. As the time changes from 1 second to 1.2 second and the isolation changes from 0.6 kW/m^2 to 1 kW/m^2. Hence, the MPPT changes from 14 W to 24.5 W. Fig.9 shows the tracking condition of the controller as the temperature changes. As the time changes from 2 second to 2.2 second and the temperature changes from 25 $°C$ to 50 $°C$. Hence, the MPPT changes from 25 W to 23 W. Fig.10 shows the tracking condition of the controller as the illumination changes.

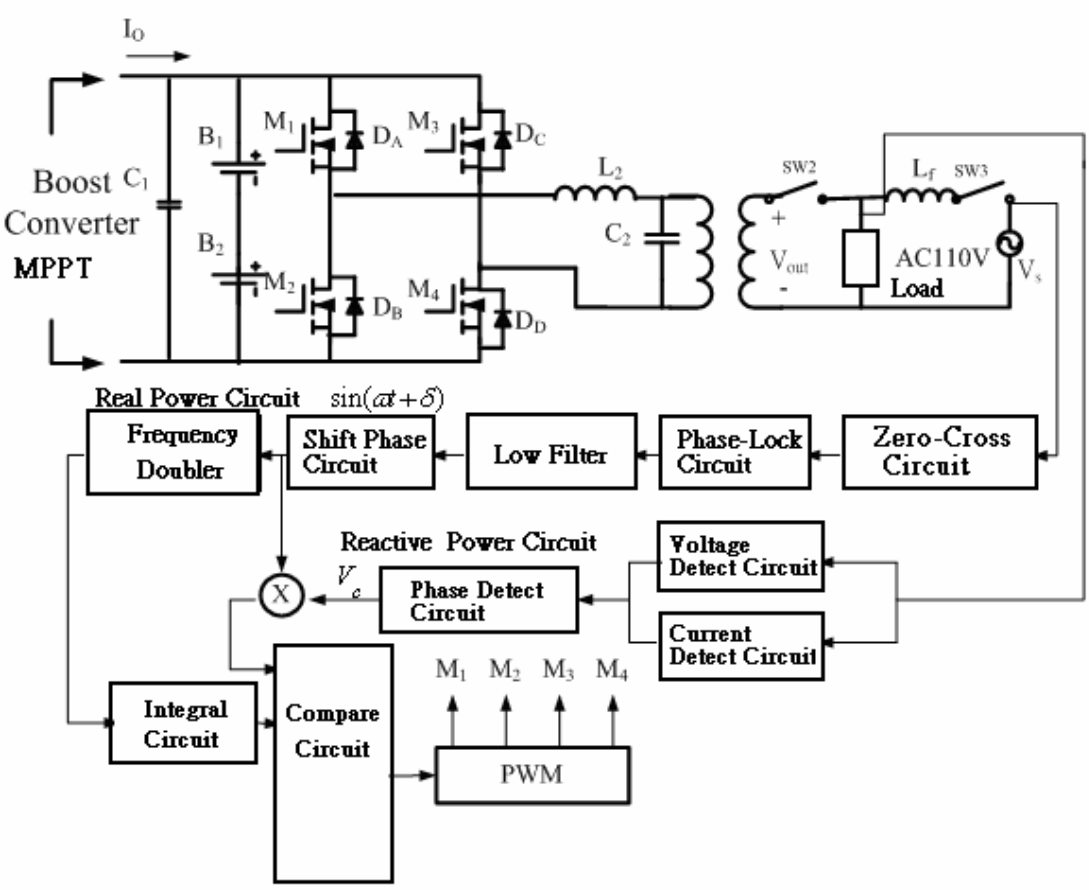

Fig. 6 The achievement of real power and reactive power

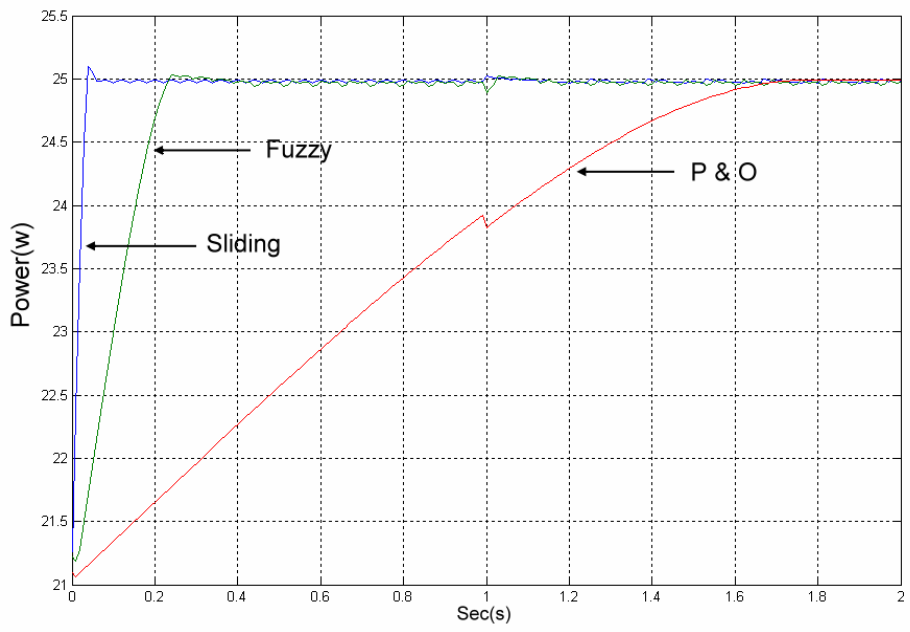

Fig. 7 The system output power ($1\,kW/m^2, 25\,^{\circ}C$)

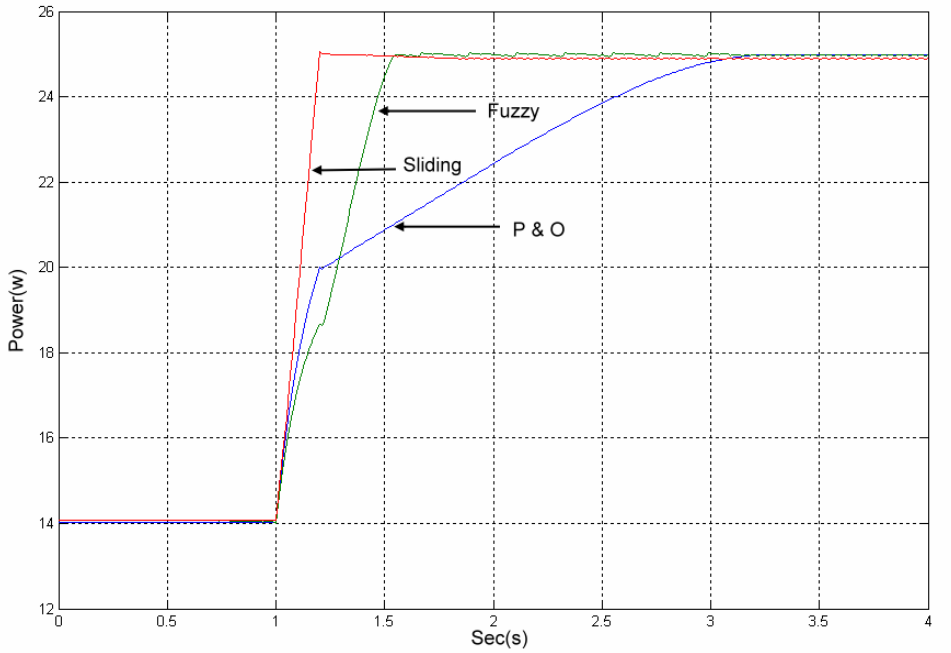

Fig. 8 The system output power (illumination change)

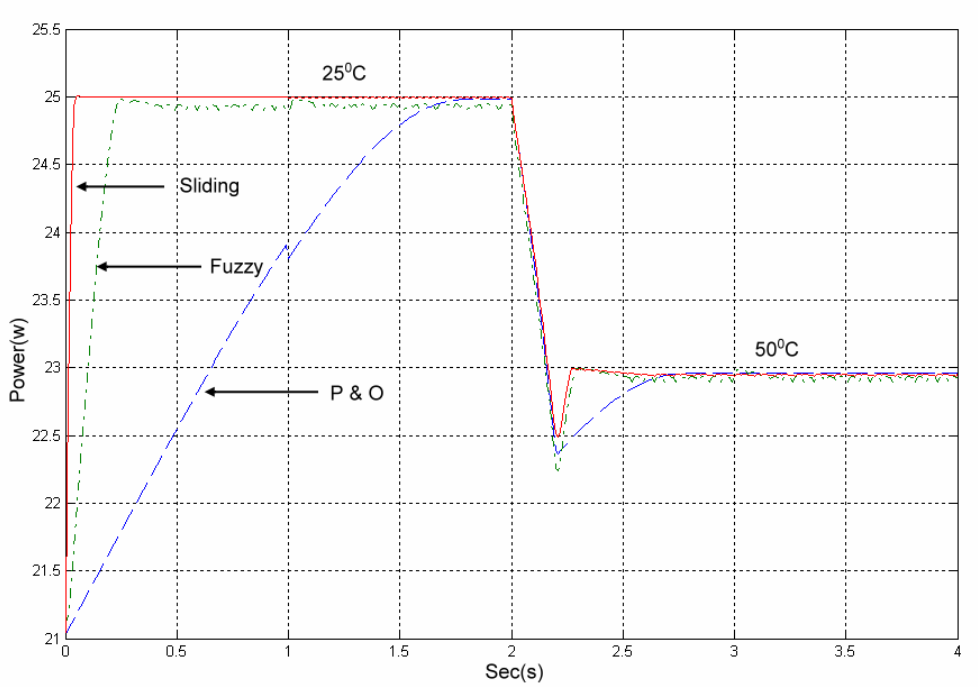

Fig.9 The system output power (temperature change)

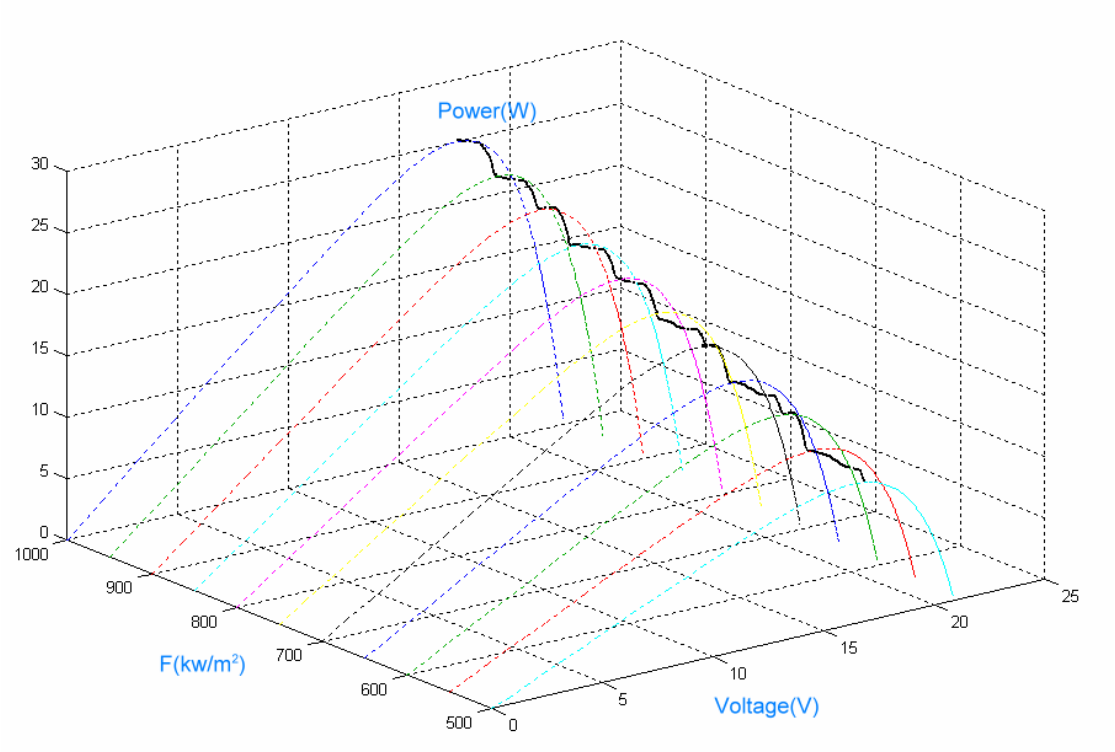

Fig. 10 Sliding algorithm of tracking maximum power point tracker

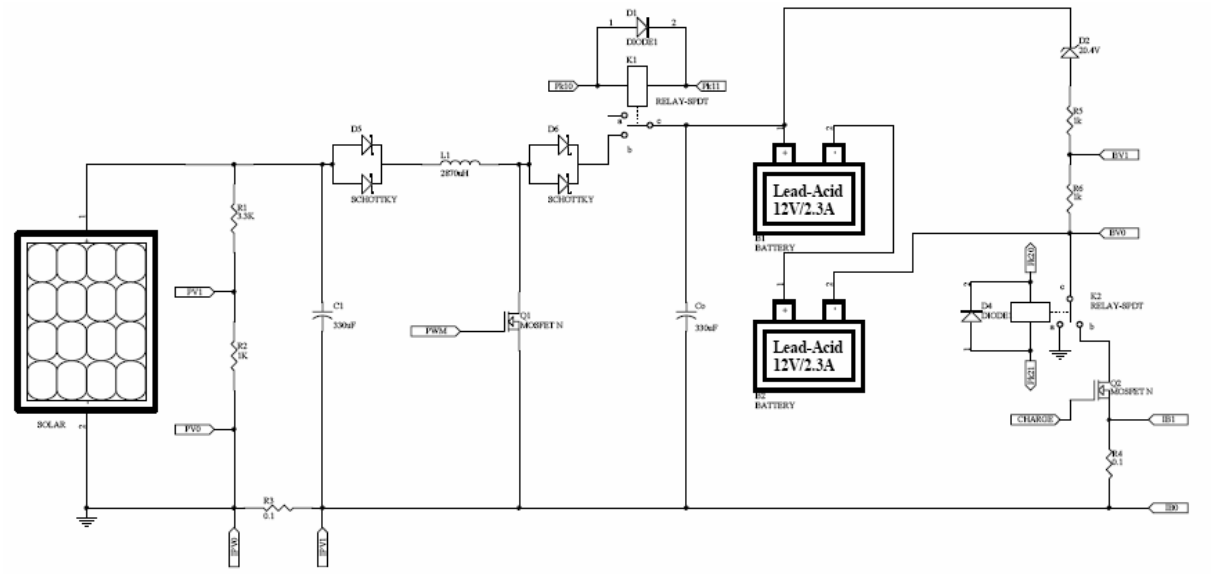

Fig. 11 Diagram of photovoltaic charger system

6.2 Experiment

Fig.11 shows the control architecture, the control system comprises Microcontroller PIC16F877A, MOSFET, L etc. Fig.12 shows the photovoltaic system. DC/DC is the charge tracking the maximum power. The storage battery is as the load. Fig.12 shows the photovoltaic system of MPPT. $T_{P\&O} = 85.9\,\text{sec}$, $T_{Fuzzy} = 16.3\,\text{sec}$, $T_{sliding} = 8.2\,\text{sec}$. Fig.13 shows pulse width module is 0.2 and charge current is 0.1A. Fig.14 shows pulse width module is 0.8 and charge current is 0.5A. By adjust the pulse width module it can get the best charger method. Fig. 15 shows zero-cross circuit of output plot. The phase-lock circuit demonstrates the circuit can track for the city power of frequency 63Hz (in Fig. 16). Fig. 16 , 17, 18 show the phase-lock circuit the circuit can track the city power of 60 Hz, 57Hz, 63Hz.. Fig.12 shows the photovoltaic system of MPPT. $T_{P\&O} = 85.9\,\text{sec}$, $T_{Fuzzy} = 16.3\,\text{sec}$, $T_{sliding} = 8.2\,\text{sec}$

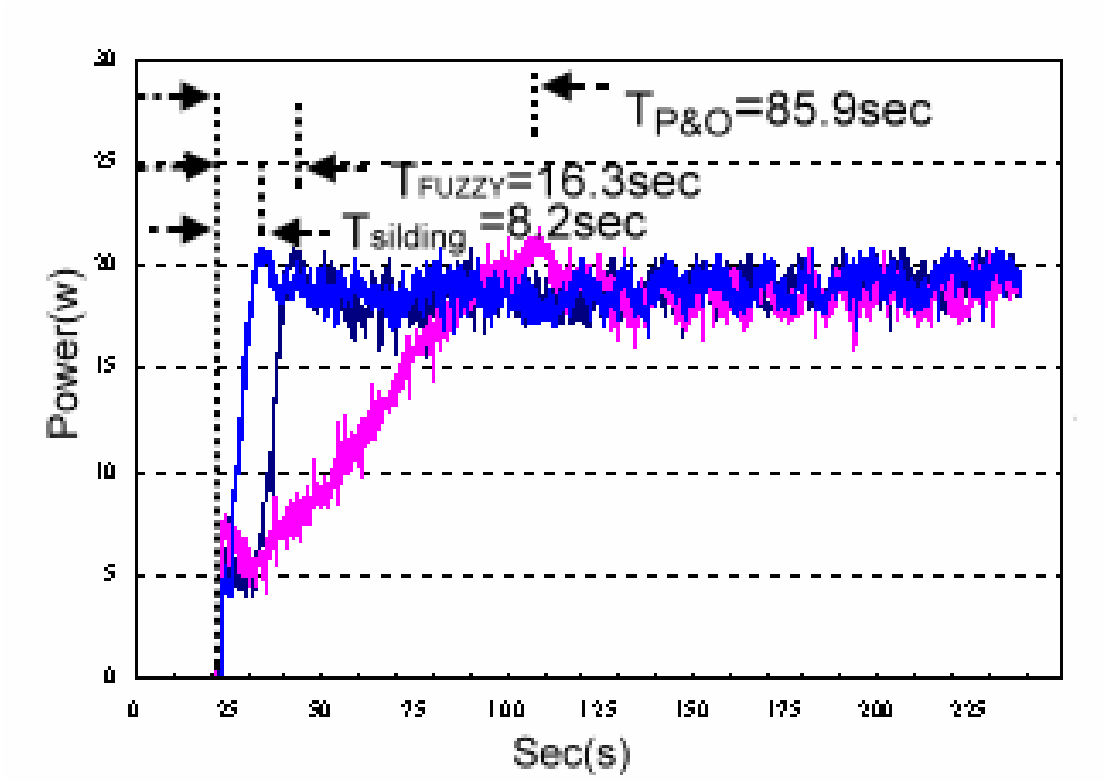

Fig. 12 P&O, Fuzzy, Sliding charge curve

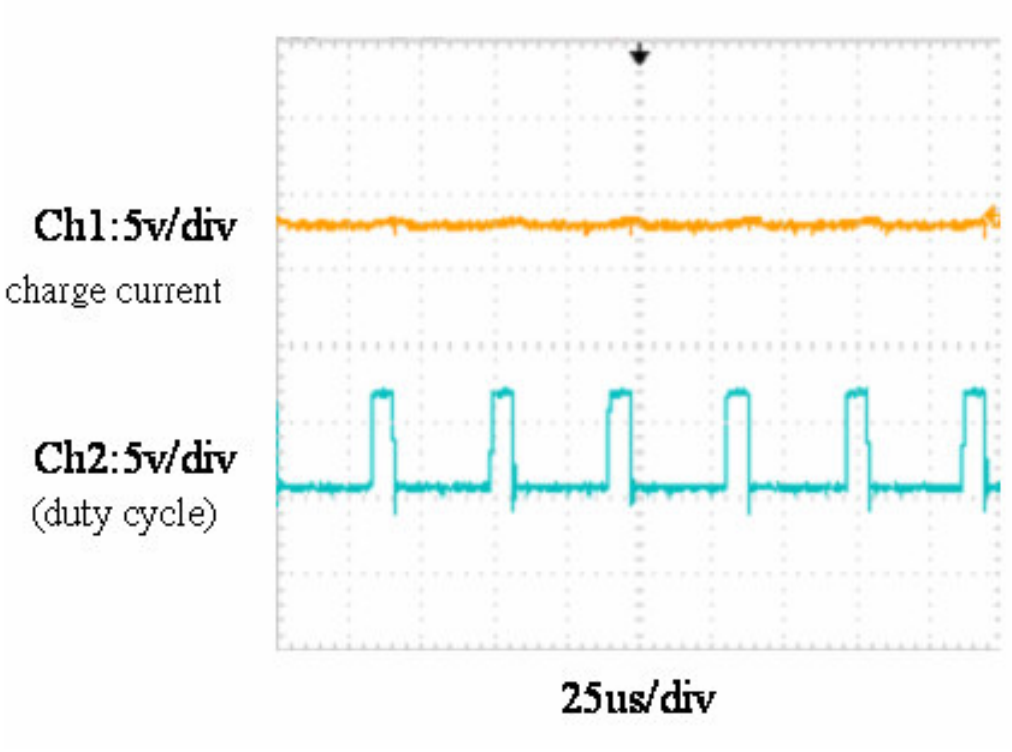

Fig. 13 D=0.2 and charge current=0.1A

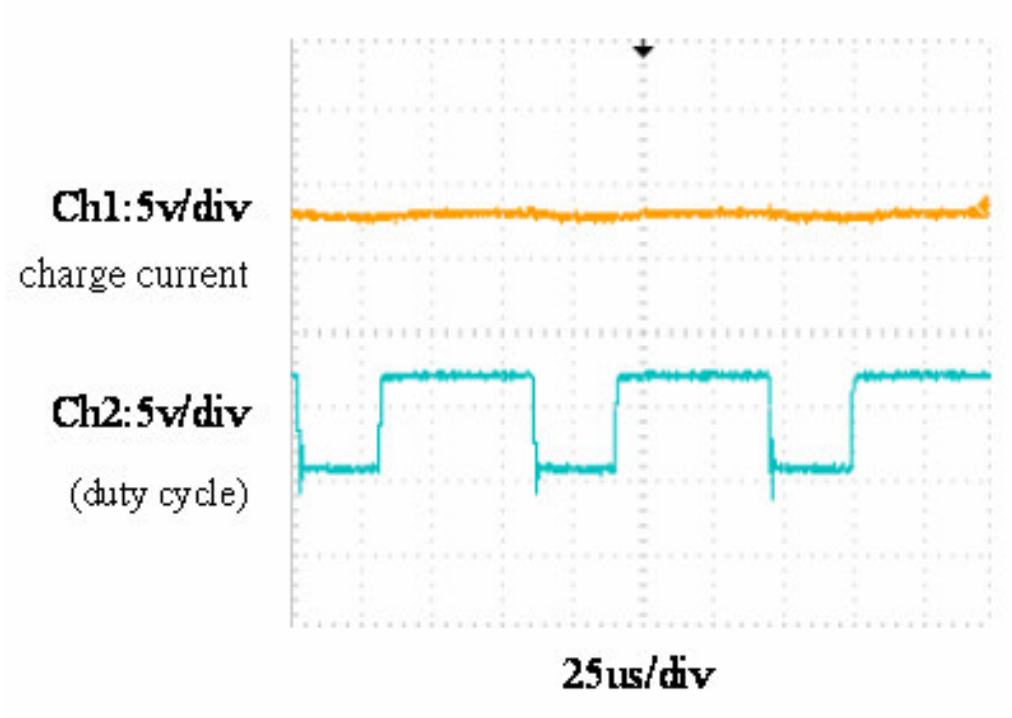

Fig. 14 D=0.8 and charge current=0.5A

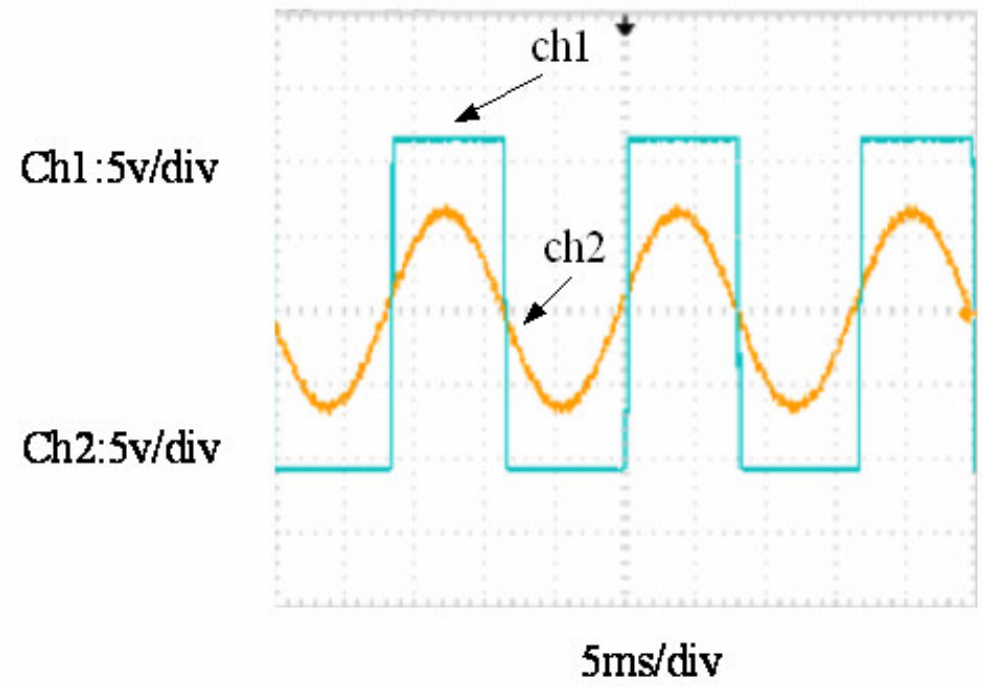

Fig. 15 The zero-cross circuit of output plot

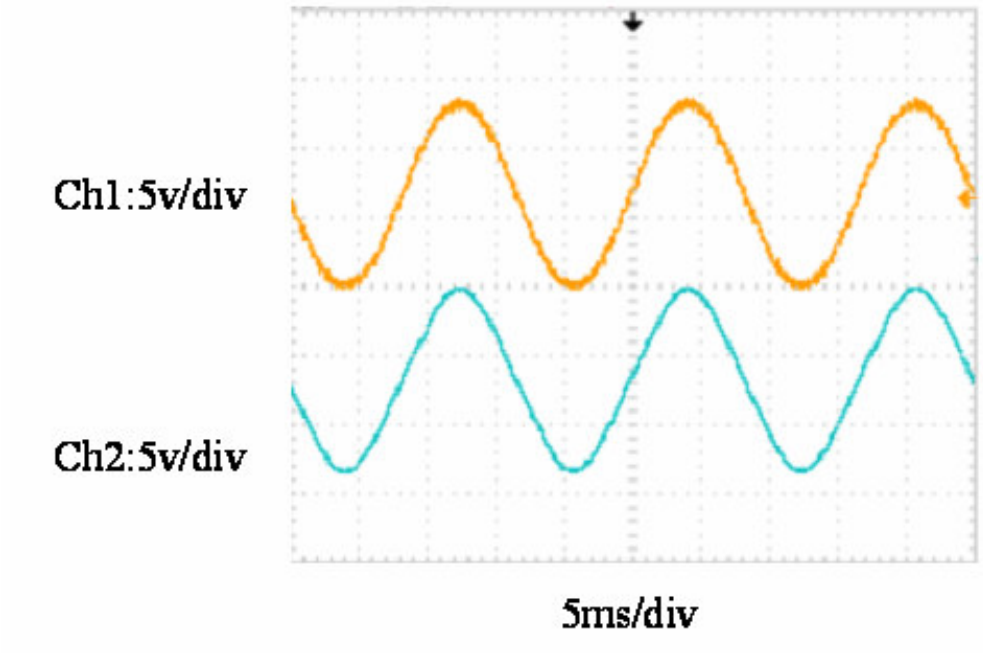

Fig. 16 The phase-lock circuit tracking for 60 Hz plot

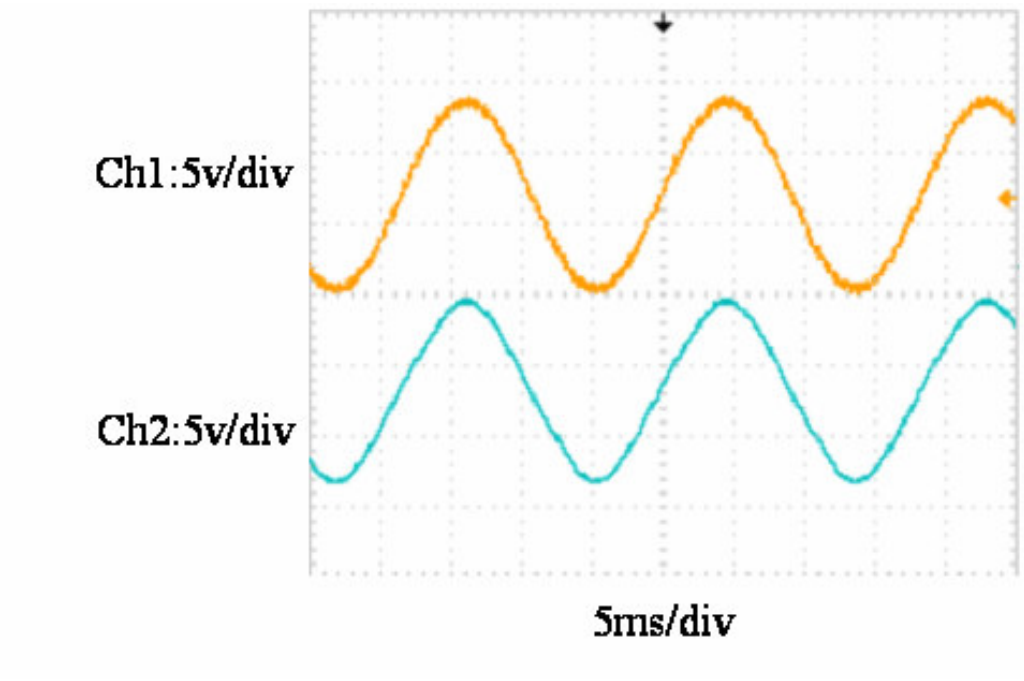

Fig. 17 The phase-lock circuit tracking for 57 Hz plot

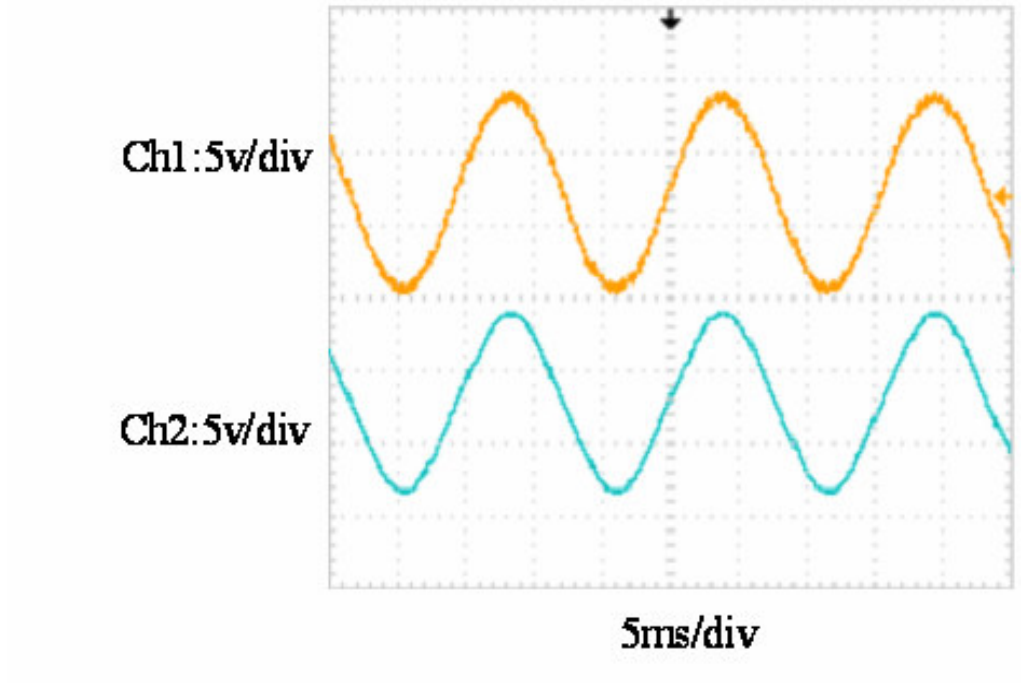

Fig. 18 The phase-lock circuit tracking for 63Hz plot

7 Conclusions

This paper presents the sliding mode controller from VSC that controls Booster type converter of solar array and battery charger to compete the tracking of MPP. After using Matlab/Simulink to simulate P&O control, fuzzy control and sliding control, compare its response time. According to the fig.3, the PV maximum power point tracking (MPPT) speed is faster apparently comparing the P&O and fuzzy control method. Seen from the simulating result, figure 4, 5 and 6, it is obvious that the efficiency of the PV MPPT is greatly improved the system shown implements the sliding control algorithm. In order to prove the feasibility of the sliding control method; a system of PV arrays was designed as fig.7 and 8. In the control system comprises Micro-controller, IC16F877A, IGBT, L etc. Experimental results show the response time of the proposed sliding control is better than P&O and fuzzy control. This paper, consisting of a Boost type dc/dc converter, which micro-processor, PIC16F877A, is used to implement the sliding mode controller. Comparing with other techniques used in the past, the use of the proposed MPPT control improves the PV system performance. The results of simulation and experiment are present.

A grid-connected inverter is designed to transform the maximum output power into the load and utility. The real power control is using zero-cross and phase-lock circuits that control the inverter output voltage which is phase lead and synchronized with the utility. A digital circuit is used to detect the phase angles of the load voltage and current to control the inverter output amplitude to achieve the reactive power load compensation. A monitor circuit is designed to detect the voltage and frequency variation in the utility. When the photovoltaic system encounters a voltage and frequency deviation, the monitor circuit immediately disconnects the photovoltaic system from the utility to prevent the island effect. The proposed system is implemented by using OP amplifiers and micro controller (PIC16F877A). Both the simulation and experimental results using MATLAB show the sliding mode controller for maximum power tracking has good performance. The phase and amplitude control experiments achieve the real and reactive power control. The island effect experiments demonstrate evidence of the solar cell system protection ability illustrating the proposed grid-connected photovoltaic system has good operating performance.

References:

[1] W. Xiao and W. G. Dunford, "A modified adaptive hill climbing MPPT method for photovoltaic power system,," *in 35th Annual IEEE Power Electron. Specialists Conf.*, 2004, pp. 1957-1963.

[2] N. Femia, G. Petrone, G. Spagnuolo, and M. Vitelli, "Perturb and Observe MPPT Technique Robustness Improved," *IEEE International Symposium on Industrial Electronics*, vol. 2, May 2004,pp.845 – 850.

[3] N. Femia, G. Petrone, G. Spagnuolo, and M. Vitelli, "Optimization of Perturb and Observe Maximum Power Point Tracking Method, "*IEEE Transactions On Power Electron.,* vol. 20, July 2005, pp. 963-973.

[4] N. Kasa. T, Iida. and L, Chen, "Flyback Inverter Controlled by Senseless Current MPPT for Photovoltaic Power System," *IEEE Trans. Iind. Electron.,* vol, 52, pp, 1145-1152,AUG, 2005.

[5] K. Kobayashi, I. Takano, and Y. Sawada, "A study on a two stage maximum power point tracking control of a photovoltaic system under partially shaded insolation conditions, "*in IEEE Power Eng. Society General Meeting,* 2003, pp.2612-2617.

[6] W. Wu, N. Pongratananukul, W. Qiu, K. Rustom, T. Kasparis, and I. Batarseh, "DSP-based multiple peak power tracking for expandable power system, "*in Eighteenth Annual IEEE Appl. Power Electron. Conf. and Exposition,* 2003, pp.525-530.

[7] T. Noguchi, S. Togashi, and R. Nakamoto, "Short-current photovoltaic power generation system, *"in Proc. 2000 IEEE International Symp. on Ind. Electron.*, 2000, pp. 157-162.

[8] N. Mutoh, T. Matuo, K. Okada, and M. Sakai, "Prediction-dada-based maximum-power-point-tracking method for photovoltaic power generation system," *in 33rd Annual IEEE Power Electron. Specialists Conf., 2002*, pp. 1489-1494.

[9] M. A. S. Masoum and H. Dehbonei. E. F. Fuchs, "Theoretical and Experimental Analyses of Photovoltaic Systems with Voltage and Current-based Maximum Power-point Tracking," *IEEE Transactions on Energy Conversion*. vol. 17, Issue 4, Dec. 2002, pp. 514-522.

[10] B. M. Wilamowski and X. Li, "Fuzzy System Based Maximum Power Point Tracking for PV System," *IEEE Annual Coufereuce of the Industrial Electronics Society,* Vol4, Nov. 2002,pp. 3280-3284.

[11] A. Tariq and M. S. Jami Asghar, "Development of an Analog Maximum Power Point Tracker for Photovoltaic Panel," *International IEEE Annual Conference on Power and Electronics and Drives Systems,* Vol.1, Jan. 2006, pp.251-255.

[12] R. A. Decarlo and S. H. Zak. G. P. Matthews, "Variable Structure Control of Nonlinear Multivariable System: A tutorial," *Proceedings of the IEEE,* Vol.76, March. 1988,pp. 212-232.

[13] J. J. Negroni; C. Meza; D. Biel; F. Guinjoan; "Control of a buck inverter for grid-connected PV systems: a digital and sliding mode control approach," *Industrial Electronics, 2005. ISIE 2005. Proceedings of the IEEE International Symposium on* Volume 2, 20-23 June 2005 Page(s):739 - 744 vol. 2

[14] A. F. Filippov, *Differential Equation with Discontinuous Rightsides,* Kluwer Academic, Dordrecht, Boston, London, 1988.

[15] E. Baily and A. Arapostathis, "Simple sliding mode control scheme applied to robot manipulator," *Int. J. of Systems Science,* Vol. 17, pp. 876-885, 1986.

[16] I. Lagrat, H. Ouakka, and I.Boumhidi," Sliding Mode PI Controller for Nonlinear Systems," *Proceedings of the 6th WSEAS International Conference on Simulation, Modelling and Optimization, Lisb*on, Portugal, September 22-24, 2006.

[17] T. J.Mabnoto, K. Sopian, W. R. W. Daud, M. Agoul and A. Zaharim," Mathematical Model for Determining the Performance Characteristics of Muti-Crytalline Photovotaic Modules", *Proc. of the 9th WSEAS Int. Conf. on Mathematical and Computational Methods in Science and Engineering, Trinidad and Tobago*, November 5-7, 2007.

[18] D. Wu and Z. Wang, " Study on Model and Control System of Variable-Speed Pitch-Controlled Wind Turbine," *Proceedings of the 7th WSEAS international Conference on Simulation, Modeling, and Optimization, Beijing, China,,* September 15-17, 2007